

2015-04-24

Distinct lower visual field preference for object shape

KANG, JUNGHEE

<http://hdl.handle.net/10026.1/10193>

10.1167/15.5.18

Journal of Vision

Association for Research in Vision and Ophthalmology (ARVO)

All content in PEARL is protected by copyright law. Author manuscripts are made available in accordance with publisher policies. Please cite only the published version using the details provided on the item record or document. In the absence of an open licence (e.g. Creative Commons), permissions for further reuse of content should be sought from the publisher or author.

Distinct lower visual field preference for object shape

McGill Vision Research, Department of Ophthalmology,
McGill University, Montreal, QC, Canada

Gunnar Schmidtman

Department of Life Sciences,
Glasgow Caledonian University, Glasgow, UK



Bradford School of Optometry and Vision Science,
University of Bradford, Bradford, UK

Andrew J. Logan

Department of Life Sciences,
Glasgow Caledonian University, Glasgow, UK



Graeme J. Kennedy

Department of Life Sciences,
Glasgow Caledonian University, Glasgow, UK



Gael E. Gordon

Department of Life Sciences,
Glasgow Caledonian University, Glasgow, UK



Gunter Loffler

Department of Life Sciences,
Glasgow Caledonian University, Glasgow, UK



Humans manipulate objects chiefly within their lower visual field, a consequence of upright posture and the anatomical position of hands and arms. This study tested the hypothesis of enhanced sensitivity to a range of stimuli within the lower visual field. Following current models of hierarchical processing within the ventral stream, discrimination sensitivity was measured for orientation, curvature, shape (radial frequency patterns), and faces at various para-central locations (horizontal, vertical, and main diagonal meridians) and eccentricities (5° and 10°). Peripheral sensitivity was isotropic for orientation and curvature. By contrast, observers were significantly better at discriminating shapes throughout the lower visual field compared to elsewhere. For faces, however, peak sensitivity was found in the left visual field, corresponding to the right hemispheric localization of human face processing. Presenting head outlines without any internal features (e.g., eyes, mouth) recovered the lower visual field advantage found for simple shapes. A lower visual field preference for the shape of an object, which is absent for more localized information (orientation and curvature) but also for more complex objects (faces), is inconsistent with a strictly feed-forward model and poses a challenge for multistage models of object perception. The distinct lower visual field preference for contour shapes is, however, consistent with an asymmetry at intermediate

stages of visual processing, which may play a key role in representing object characteristics that are particularly relevant to visually guided actions.

Introduction

Historically, neurons at the early stages of visual processing in primary visual cortex (V1) were thought to act like filters, which are tuned to contour orientation and spatial frequency (SF) (Hubel & Wiesel, 1962; Hubel & Wiesel, 1968). More recent work has revealed a more complex picture of nonlinear behavior that depends on stimulation from within as well as outside the classical receptive field, including contrast normalization, long-range interactions, surround suppression, and cross-orientation inhibition (Carandini & Heeger, 2011; see Loffler, 2008, for review). Beyond V1, processing follows two prominent pathways: the dorsal and the ventral stream (Goodale & Milner, 1992; Ungerleider & Mishkin, 1982). Along these pathways, the receptive fields of neurons enlarge systematically as neurons become selective for features of increasing complexity (Logothetis, Pauls, & Poggio, 1995; Tanaka & Kobatake, 1994). At intermediate

Citation: Schmidtman, G., Logan, A. J., Kennedy, G. J., Gordon, G. E., & Loffler, G. (2015). Distinct lower visual field preference for object shape. *Journal of Vision*, 15(5):18, 1–15, <http://www.journalofvision.org/content/15/5/18>, doi:10.1167/15.5.18.

stages of the ventral pathway in V2 and V4, neuronal responses exhibit behavior that is consistent with the integration of information from early detectors (Gallant, Connor, Rakshit, Lewis, & Van Essen, 1996; Hegdé & Van Essen, 2007; Pasupathy & Connor, 2002; Yau, Pasupathy, Fitzgerald, Hsiao, & Connor, 2009). Recordings from macaque V2 are consistent with processing of curvature and angles (Hegdé & Van Essen, 2000; Ito & Komatsu, 2004) by combining outputs from multiple orientation-selective neurons in the striate cortex. At the next level, neurons in V4 exhibit selectivity for curved shapes, including concentric circles (Dumoulin & Hess, 2007; Gallant, Braun, & Van Essen, 1993; Wilkinson et al., 2000), which requires pooling of information from detectors tuned to a wide range of orientations centered at different positions within the visual field (VF). At the highest level along the ventral stream, neurons in the infero-temporal cortex are selective for complex shapes and objects (Logothetis et al., 1995), including faces (Kanwisher & Yovel, 2006; Tsao & Livingstone, 2008). Given this progressive increase of processing complexity, it has been proposed that the organization of the ventral visual stream is both distributed and hierarchical: Global shape representations at intermediate stages integrate signals from the early stages tuned to contour parts. In turn, representations of contour shape may provide input to more complex object coding at the highest levels (Cadiou et al., 2007; Loffler, 2008, 2015; Loffler, Wilson, & Wilkinson, 2003; Riesenhuber & Poggio, 2000; Schmidtman, Kennedy, Orbach, & Loffler, 2012; Van Essen, Anderson, & Felleman, 1992).

Such distributed coding strategies allow for specialization that may be particularly relevant for certain visual tasks, for example, object manipulation. Primate species rely on the detection of objects below eye level, i.e., that are predominantly located in the lower part of their VF. That is, objects will initially appear in the lower VF before they are manipulated, and a higher sensitivity for shape in the lower peripheral field will enable more accurate reaching and grasping that might be followed and further refined by subsequent foveal fixation. There are instances in everyday viewing conditions in which objects are effortlessly manipulated peripherally without fixation, for instance, changing a gear while driving or reaching for a glass of wine during a conversation. Correspondingly, a lower VF specialization has been proposed for grasping and tool manipulation (Previc, 1990), and this has been confirmed for human visuomotor control (Rossit, McAdam, Mclean, Goodale, & Culham, 2013). It has been argued that the preference for the lower VF is essentially linked to visually guided action because passive viewing of stimuli does not result in differential activity for lower versus upper VF targets (Previc, 1990).

It is well established that visual perception depends on the location within the VF with sensitivity decreasing with eccentricity (Strasburger, Rentschler, & Jüttner, 2011). The effect of eccentricity on sensitivity is not homogeneously distributed across the visual field. Behavioral studies have found performance at the same eccentricity to be better along the horizontal meridian (left and right VF) than at locations along the vertical meridian: the horizontal–vertical anisotropy (HVA; Abrams, Nizam, & Carrasco, 2012). Along the weaker vertical axis, better performance has been reported for the lower compared to upper VF (vertical meridian asymmetry; VMA). For example, Rubin, Nakayama, and Shapley (1996) used illusory contours to show that figure–ground segregation is better in the lower VF compared to the upper VF. The VMA is generally restricted to the vertical meridian and absent for intercardinal axes (e.g., $\pm 45^\circ$ relative to vertical; Abrams et al., 2012).

The behavioral HVA is mirrored anatomically by an over-representation of the horizontal compared to the vertical meridian at the level of the retina (cone mosaic and retinal ganglion cells; Curcio & Allen, 1990), in the magnocellular layers of the lateral geniculate nucleus (LGN) (Connolly & Van Essen, 1984), in V1 (Tootell et al., 1998; Van Essen, Newsome, & Maunsell, 1984; cf. Adams & Horton, 2003), and extrastriate area MT (Maunsell & Newsome, 1987). Although physiological evidence has been presented in support of the behavioral VMA (Liu, Heeger, & Carrasco, 2006; Portin, Vanni, & Virsu, 1999), anatomical evidence is less compelling. A marginal over-representation of the lower versus upper VF has been shown at the retina, LGN, and V1 (Connolly & Van Essen, 1984; Curcio & Allen, 1990; Curcio, Sloan, Packer, Hendrickson, & Kalina, 1987; Tootell et al., 1998; Van Essen et al., 1984; but see Adams & Horton, 2003), but, unlike perception, these anatomical findings are not generally narrowly restricted to the vertical axis (Abrams et al., 2012).

The pattern of highest sensitivity along the horizontal compared to the vertical meridian (HVA) and its anatomical correlates is at odds with the hypothesis of a lower VF advantage for human tool manipulation (Previc, 1990) and the superior performance for visually guided action in the lower VF (Danckert & Goodale, 2003). This poses the question as to the source of this enhanced reaching and grasping performance and whether a lower VF advantage may simply not be observed for “passive” visual perception tasks that do not require visually guided actions.

The present study tested an alternative hypothesis that the lower VF advantage for object manipulation may rely predominantly on processing the shape of objects and may, therefore, become manifest only for certain visual tasks specific to shape coding. Other visual tasks, including those that have been used in

earlier studies (Abrams et al., 2012; Hay, 1981; Leehey, Carey, Diamond, & Cahn, 1978; Young, Hay, McWeeny, Ellis, & Barry, 1985), may not elicit a lower VF preference.

This hypothesis was tested by systematically investigating visual sensitivity for stimuli of increasing complexity at various locations and para-central eccentricities within the peripheral VF. Following the hierarchical processing of visual information in the ventral stream, observers ability to discriminate “contour parts,” i.e., the orientation or curvature of segments (low-level tasks); “object shapes” (midlevel); and “complex objects,” i.e., faces (high-level) were measured.¹ Superior performance in lower VF locations was observed only for object shape.

Materials and methods

Participants

For the experiments on orientation, curvature, and shape discrimination, two psychophysically experienced observers (one naïve) and a further four naïve participants were recruited. Three of these observers (two naïve) took part in the face-discrimination experiment. All observers had normal or corrected-to-normal visual acuity. None of the subjects had visual field defects (confirmed by a Humphrey C40—Carl Zeiss Meditec—visual field test, which tests the integrity of the central 30° of the visual field). Observations were made under binocular viewing conditions in a well-lit room. No feedback was provided. Informed, written consent was obtained from each observer, and the study was approved by Glasgow Caledonian University’s Life Sciences Ethics Committee. All experiments were conducted in accordance with the Declaration of Helsinki.

Apparatus

Stimuli were generated within the Matlab environment and presented using routines from the Psychtoolbox extensions (Pelli, 1997) on a LaCie high-resolution monitor (1024 × 768 at 85 Hz; mean luminance 61 cd/m²) controlled by a Mac mini computer. At the test distance (0.8 m if not stated otherwise), the monitor subtended 25.4° by 19.6° of visual angle and one pixel subtended 0.026°.

Stimuli

(a) Orientation discrimination: Line segments (profile of a fourth derivative of Gaussian—D4; Loffler et al., 2003; Schmidtman et al., 2012; Wilkinson,

Wilson, & Habak, 1998) of variable orientations were used to determine orientation discrimination. The spatial extent of the stimulus was defined to match the chord of a circular segment (angular extent 72°) used for curvature discrimination (see below). A single Gaussian window (sigma = 0.4°) was applied to ramp down the contrast on each side of the D4 line. The line length, defined as the distance between points at which the Gaussian reaches half its maximum value, was 0.5° in central vision. The width of all stimuli, defined as the distance between the points at which the D4 luminance profile reaches half its height, was 0.025° centrally. The orientation of the reference pattern was typically vertical.

- (b) Curvature discrimination: Circular segments (D4 profile) of variable radius were used to determine curvature discrimination. These stimuli were defined analogous to the shapes (see below) as radial frequency patterns with a modulation amplitude of zero (circle). In order to extract circular segments, the contrast of the circular contour was modulated along its circumference by a Gaussian (Schmidtman et al., 2012). The angular extent of the Gaussian was set to 72° (one fifth of a full circle). The radius of the reference pattern was 0.5° (baseline curvature of 2.0°). The segment length was randomly varied by ±10% of the reference angular extent of 72° to avoid additional cues to the task, such as estimation of chord length or sag.
- (c) Shape discrimination: Radial frequency (RF) patterns were used to measure shape sensitivity. RF patterns are sinusoidally modulated circular contours, defined in polar coordinates:

$$r(\theta) = r_{mean}[1 + A\sin(\omega\theta + \varphi)] \quad (1)$$

where r_{mean} represents the mean radius (size), φ the phase (orientation), ω the frequency (number of cycles or corners), and A the modulation amplitude (pointedness of each corner). The reference shape was a circle ($A = 0$). Observers were asked to discriminate the reference shape from RF patterns of varying amplitudes. Shapes with with two different radial frequencies, three and five, were used. These shapes are processed globally by integrating information from across entire contours rather than by relying on local properties, such as orientation or curvature (Loffler et al., 2003; Schmidtman et al., 2012; Wilkinson et al., 1998). RF patterns were always presented with random orientation (phase) so that the exact location of specific contour parts was unpredictable.

- (d) Face discrimination: Synthetic faces were used to measure face discrimination. The design of synthetic faces has been described in detail elsewhere (Wilson, Loffler, & Wilkinson, 2002). Briefly, major geomet-

ric face information was digitized at 37 points (e.g., external head contour and feature shape/position) from gray-scale face photographs with neutral expressions. A polar coordinate grid was superimposed on the face photograph, centered on the bridge of the nose. The external contour of the head was measured at 16 locations angularly positioned at equal intervals of 22.5° . The polar coordinates of 14 of the measured points were used to define seven RFs to interpolate the subject's head shape. A further nine points were utilized to define four RFs that captured the shape of the hairline. The internal face features (nose, mouth, eyes, and eyebrows) were defined by 14 additional measurements (e.g., width of the lips, length of the nose). These measurements were used to adjust generic features in width and length to reflect those of the subject. The shape of the eyes and eyebrows, on the other hand, was identical in all synthetic faces. Individuating information was contained within variations in horizontal and vertical eye position, in addition to the height of the eyebrows, defined relative to the center of the eyes. Each of these 37 parameters was utilized to define a 37-dimensional vector, which completely describes an individual face.

All faces were scaled to the same size by normalizing face measurements by the ratio between individual head radius and mean radius. At the test distance of 0.8 m, each face subtended 8.2° of visual angle. The geometric difference between two faces was calculated as the Euclidean distance between their two 37-dimensional vectors. The vector representing a face was normalized to produce a specified geometric difference relative to the mean head radius (percentage of face geometry). This geometric difference quantifies the distinctiveness of individual faces and captures discrimination sensitivity (Wilson et al., 2002). The synthetic faces were then band-pass filtered at the optimal SF for face identification (difference of Gaussian filter of 2.0 octave bandwidth centered upon a peak SF of 10 cycles/face width; Näsänen, 1999). The resulting faces accentuate geometric information in the most important frequency band while omitting cues such as hair and skin texture, skin color, and wrinkles.

- (e) Peripheral presentation and stimulus scaling: For central vision, discrimination thresholds for face, shape, curvature, and orientation discrimination were measured at 0° eccentricity. Performance in the peripheral VF was measured at 5° or 10° eccentricity along the horizontal and vertical meridian. For RF shapes, thresholds were also determined along the main diagonals (45° and 135°). The peak SF of the filter (faces) and D4 (RF

shapes, curvature, and line segments) was set to $8\text{ c}/^\circ$ for central vision.

The central purpose of this study was to determine how the direction of VF location affects the sensitivity to a range of stimuli, i.e., the pattern of sensitivity when presenting stimuli in different parts of the VF without changing eccentricity. We did not aim to investigate the precise magnitude of sensitivity loss when comparing central with peripheral viewing at different eccentricities nor did we try to derive appropriate scaling factors required to match peripheral sensitivity to that found centrally.

It has been well documented in the literature that, in order to achieve similar sensitivity, the presentation of stimuli in the peripheral VF requires scaling of size (increase) and SF (decrease) as a function of eccentricity. The following linear relationship has been frequently used to compensate the decrease in performance with increasing eccentricity (Strasburger et al., 2011):

$$F = 1 + E/E_2 \quad (2)$$

where the scaling factor F increases linearly in relation to eccentricity E ($^\circ$). E_2 ($^\circ$) represents the eccentricity at which the size of the stimulus must be doubled in order to achieve equivalent thresholds in the periphery (Levi, Klein, & Aitsebaomo, 1985).

Apart from eccentricity, the precise scaling factor depends on the task and the stimulus as well as VF location. Regarding the latter, in the presence of, e.g., a HVA, a different scale factor would be required for horizontal compared to vertical VF locations even for the same task. Rather than using different factors for different conditions, we decided to use the same scaling factor of $E_2 = 2.5^\circ$, which is the average value across a range of visual tasks and studies as reviewed by Strasburger et al. (2011).

Accordingly, all dimensions of the stimuli for orientation, curvature, and shape discrimination (SF, size, length, and positional jitter) were scaled by setting $E_2 = 2.5^\circ$ in Equation 2. The circular curvature segments and the RF patterns with r_{mean} of 0.5° and peak SF of $8\text{ c}/^\circ$ in central vision were scaled to 1.5° and $2.67\text{ c}/^\circ$ at 5° eccentricity and 2.5° and $1.6\text{ c}/^\circ$ at 10° eccentricity, respectively. The width of the stimuli, defined as the distance between the points at which the D4 luminance profile reaches half its height, was 0.025° centrally and scaled to 0.075° and 1.252° for 5° and 10° eccentricity, respectively. The length of the line segments for orientation discrimination was scaled from 0.5° in central vision to 2.385° at 10° eccentricity. Our data (see below) show that this scaling is appropriate for orientation and curvature discrimination but overestimates peripheral sensitivity for shape discrimination.

With regards to face discrimination, it has been shown that central face discrimination for the synthetic faces used in our study is scale invariant (Wilson et al.,

2002). This is perhaps not surprising as the metric used to describe sensitivity is relative to the size of the faces. Therefore, the peripheral stimuli were not scaled relative to those used centrally. In a control condition on two of the observers participating in the present study, central face discrimination thresholds were unaffected by reducing the size of the synthetic faces by a factor of five. Hence, our results, in terms of threshold elevations between peripheral and central presentation, would have been unchanged had we used smaller faces centrally. In other words, we would have obtained the same threshold elevations with a scaling factor between one and five. Most importantly, the pattern of peripheral sensitivity as a function of VF location is, for all tasks and stimuli, unaffected by scaling. Hence, the overall conclusions (see below) are independent of the scaling used.

In order to ensure that the stimuli were identical for different conditions and to avoid monitor distortion effects, the stimuli were always presented at the center of the screen. Different locations within the VF were tested by presenting a circular white fixation dot subtending 7 pixels (0.186°) at either 5° or 10° eccentricity along the vertical, horizontal, or diagonal meridians. For example, to test the right VF, the fixation dot appeared on the left side of the screen. The eccentricity was measured from the center of the faces, the center of the RF patterns, or the center of the vertical D4 lines. For curvature discrimination, the apex of the circular segment was the point from which the eccentricity was calculated. For the curvature discrimination experiment, the viewing distance was reduced to 0.6 m to allow stimuli to be presented at 10° eccentricity. The parameters of the curvature segments were scaled accordingly.

Procedure

All the experiments employed the method of constant stimuli within a two-interval forced choice paradigm. In all experiments, observers had to identify which interval contained the target that differed from a reference stimulus. Observers indicated their decision by pressing one of two keys on a computer keyboard.

The reference for orientation discrimination was a vertical line. The target was a nonvertical line, which was randomly tilted in a clockwise or counterclockwise direction. The reference for curvature discrimination was a circular segment of 0.5° radius; the targets contained a higher curvature segment, i.e., smaller radius. The reference for shape discrimination was a circular contour, and the targets differed in RF amplitude. The reference for face discrimination was the average/mean face. Observers were familiarized with this face through use of an irrelevant face-matching task in which feedback was provided prior to

data collection. Target faces differed from the mean face by variable amounts of face geometry, making them less symmetric and more caricature-like.

For orientation, curvature, and shape discrimination, six target increments were tested, selected depending on the sensitivity of the observer with a logarithmic progression of 2.0 dB. The monitor screen was initially set to a mean gray luminance. Each trial contained two stimuli, presented for 160 ms each, with an interstimulus interval of 300 ms. The order of presentation (reference or target first) and the target increment was selected randomly for each trial. Individual conditions, including VF location, were tested within one block. Each of the six increments was presented 30 times within a block, giving a total number of 180 repetitions per threshold estimate for each experimental condition.

To determine face discrimination, participants were initially trained with the mean face. The subsequent task was to discriminate between two synthetic faces: the mean face (reference) and an identity face (target) that differed from the mean face by variable amounts (distinctiveness) with respect to all of the face features (head shape, position of eyes, length of nose, etc.). The two faces were presented sequentially. A face stimulus (110 ms) was followed by a low-level, filtered binary noise mask (200 ms). An interstimulus interval (350 ms) preceded the presentation of a second face (110 ms) and was also followed by a noise mask (200 ms). Observers indicated which temporal interval contained the identity (target) face. In each trial, the identity of the (target) face was randomly selected from one of four possible male faces (untrained). The identity face was randomly assigned to the first presentation interval in 50% of trials. The magnitude of the difference between the mean and identity faces was adjusted to determine a discrimination threshold.

In addition to full faces, discrimination thresholds were also measured for external features (head shape and hairline), internal features (nose, mouth, eyes, and eyebrows), and head shapes presented in isolation. Six levels of distinctiveness (percentage of geometric difference relative to mean face) were used, selected to sample the range of the observer's sensitivity. Each level was presented 20 times, resulting in 120 trials for each threshold determination. The experiments were blocked by VF location and visible face features. Each block measured discrimination thresholds for the same four male synthetic face identities. Because discrimination thresholds did not differ between individual faces, average discrimination thresholds are presented throughout. The order of presentation of the individual identities and face distinctiveness levels was fully randomized.

The order of testing of the VF locations was balanced between observers. Subjects typically com-

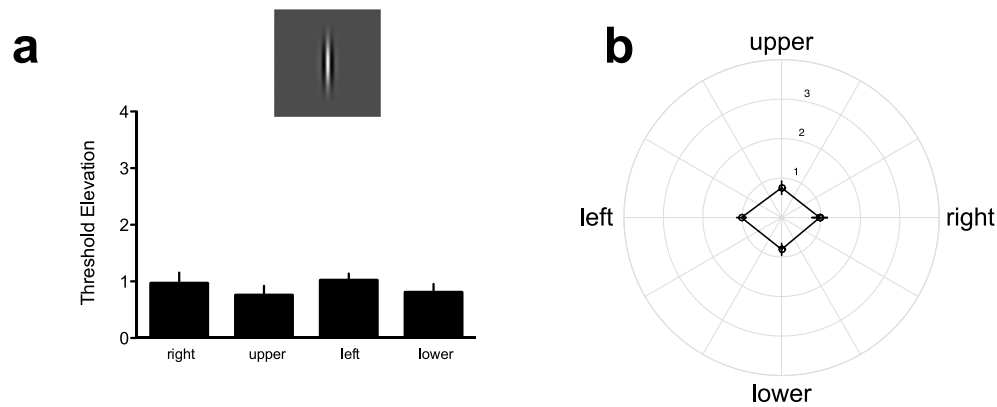


Figure 1. Low-level task: orientation discrimination at various peripheral locations. Observers were required to discriminate between a vertical target (fourth derivative of a Gaussian D4; see inset and Materials and methods) and one with a variable orientation offset. (a) A sample stimulus and the results for four observers. Performance was initially measured centrally and subsequently along the main vertical and horizontal meridians at 10° eccentricity. Data are presented as threshold elevations relative to central performance. The errors bars (here and elsewhere) represent 95% confidence intervals. With scaled stimuli, peripheral orientation discrimination sensitivity is similar to that measured centrally. Importantly, performance does not show a significant dependence on VF location. Peripheral orientation discrimination has previously been shown to be optimal if the direction of the line stimuli is arranged radially with respect to the foveal center (Davey & Zanker, 1998). We therefore repeated the experiment (data not shown) with horizontal orientations for the left/right VF location on three observers, but this did not affect sensitivity, $F(3, 9) = 0.643$; $p = 0.607$. We also determined performance with increased spatial frequency of the lines as the extent of VF asymmetries (HVA and VMA) has been shown to depend, to some extent, on spatial frequency (Skrandies, 1985). Changing the peak spatial frequency from $1.6\text{ c}/^\circ$ to $6\text{ c}/^\circ$ did not lead to a significant change in orientation discrimination (data not shown). (b) The same data as in (a) in a polar plot as a function of the tested VF location. The regular configuration of the data evidences a lack of VF asymmetry.

pleted two runs of each condition, and their results were averaged. Data for the different target increments for each condition were individually fitted by a quick function using a maximum likelihood procedure. Discrimination thresholds were defined as the point yielding 75% correct responses.

Fixation compliance for each observer was assessed with an eye tracker (Tobii Technology, Inc., Danderyd, Sweden) in a randomly selected peripheral experimental block of trials. The recordings showed accurate peripheral fixation in all cases.

Data are presented as threshold elevations relative to performance for central presentation for that condition to allow results for different conditions (tasks such as orientation, curvature, shape, and face discrimination; eccentricities; VF location) to be compared directly.

Results

Low-level tasks: Orientation and curvature discrimination

Behavioral studies on orientation discrimination have provided estimates of the bandwidth of orientation channels (Phillips & Wilson, 1984) that closely match those of neurons in macaque V1 (De Valois, Yund, &

Hepler, 1982). Hence, it has been suggested that orientation discrimination is a low-level task that is limited by activity at the early stages of visual processing.

Sensitivity to discriminating vertical line orientation was measured both centrally and peripherally at 10° eccentricity in the main horizontal and vertical meridians (with scaled stimuli; see Materials and methods) (Figure 1). The minimum orientation change that was required to distinguish between a tilted and a vertical line was comparable for peripheral (average $0.92^\circ \pm 0.118^\circ$) and central vision ($1.037^\circ \pm 0.04^\circ$). Threshold elevations (peripheral relative to central performance) did not show a dependence on VF location, repeated-measures ANOVA: $F(4, 12) = 2.042$; $p = 0.152$. This lack of VF asymmetry is evident from the polar representation of the data in Figure 1b.

We next measured curvature discrimination (Figure 2). Observers indicated which of two sequentially presented circular arcs had the higher curvature (shorter radius). Thresholds for scaled segments at 10° eccentricity are slightly elevated compared to central viewing, but, as for orientation, they do not depend on VF location, $F(4, 12) = 0.474$; $p = 0.754$.

Midlevel task: Contour shape discrimination

Evidence from behavioral (Loffler, 2008; Loffler et al., 2003; Schmidtman et al., 2012; Wilkinson et al.,

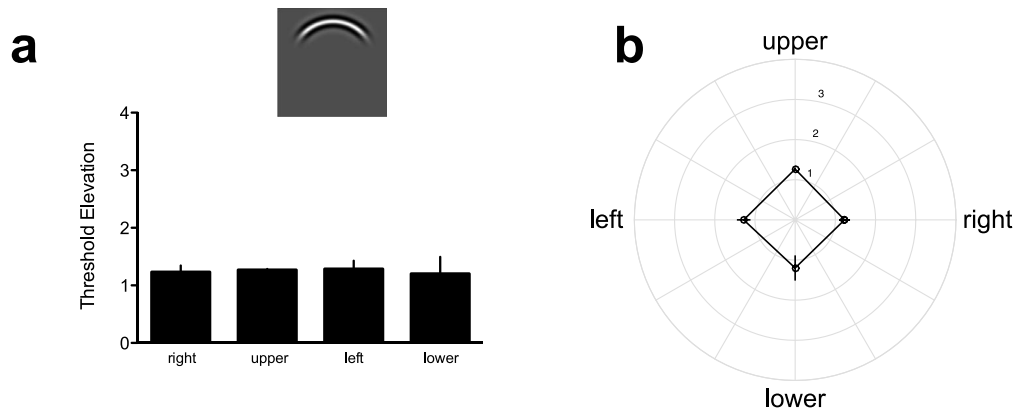


Figure 2. Low-level task: curvature discrimination at various peripheral locations. Curvature discrimination for circular segments (inset) was measured centrally and at 10° eccentricity along the horizontal and vertical meridians. The task was to indicate which of two sequentially presented stimuli contained the higher curvature. In order to avoid reference cues, such as the estimation of the chord length, sag, or aspect ratio, the length of the arc was randomly varied by $\pm 10\%$. For peripheral measurements, the arcs were always presented so as to be convex relative to fixation. (a) Performance was measured as curvature increment thresholds (1°), and data for 10° eccentricity are presented relative to the central sensitivity. As for orientation, no VF asymmetry is evident for curvature discrimination. (b) The same data as in (a) in a polar plot.

1998), neurophysiological (Gallant et al., 1996; Hegdé & Van Essen, 2007; Pasupathy & Connor, 2002; Yau et al., 2009), and imaging (Dumoulin & Hess, 2007; Wilkinson et al., 2000) studies has accumulated in favor of intermediate stages of visual processing in which information from local contour fragments is combined to represent global shape. We measured shape sensitivity by determining observer ability to discriminate closed contours (RF patterns; Wilkinson et al., 1998; see Materials and methods). These contours are parameterized with respect to their frequency (number of lobes) and amplitude (sharpness of corners). In central vision, thresholds for discriminating a circle from a shape that contains circular deformation are in the hyper-acuity range, and this exquisite sensitivity can be explained by global pooling of contour information (Loffler et al., 2003; Schmidtman et al., 2012).

Data for 5° and 10° eccentricities along the main horizontal, vertical, and diagonal meridians (45°, 135°) are presented as threshold elevations relative to central sensitivity (Figure 3) for two RF shapes (triangular: RF3; pentagonal: RF5). The difference between eccentricities was not significant, $F(1, 20) = 1.057$; $p = 0.351$. A significant difference was found, however, for VF location, $F(4, 20) = 26.122$; $p < 0.001$. Significant differences between individual conditions are indicated by asterisks in Figure 3. For both shapes and eccentricities, performance is best for the lower VF locations (lower, lower left, lower right). Performance along the horizontal meridian (right and left) is intermediate: It is consistently poorer than anywhere in the lower VF but typically better than the upper VF. Shapes presented in the lower VF are judged more accurately than at other VF locations by, on average, 56% (RF3 at 5°: 36%; RF3 at 10°: 51%; RF5 at 5°: 55%;

RF5 at 10°: 83%) and 30% (RF3 at 5°: 27%; RF3 at 10°: 44%; RF5 at 5°: 14%; RF5 at 10°: 34%) compared to the upper VF and horizontal meridian, respectively. Differences between VF locations for each shape and eccentricity were assessed statistically (repeated-measures ANOVAs with VF location as factor). The main effect of VF location was significant for all conditions ($p < 0.05$).

The pattern of behavior is independent of shape and eccentricity: Highest sensitivity (lowest threshold elevations) is seen for the lower VF quadrants (lower, lower left, lower right). Performance along the horizontal meridian (right and left VF) is consistently poorer than for the lower VF locations but typically better than for the upper VF locations. This pattern of behavior can easily be appreciated from the noncircular contour plots in Figure 3b. Hence, we observe superior performance when target shapes are presented in all of the tested lower VF locations rather than a HVA (which would result in better performance horizontal compared to vertical) or VMA (which would result in better performance inferior compared to superior but limited to the vertical midline; Abrams et al., 2012).

In summary, RF pattern discrimination performance is best in the lower VF. This extends across the entire lower VF tested, i.e., at least $\pm 45^\circ$ beyond the vertical meridian with performance better in the lower VF than along the horizontal dimension. Given the lack of VF asymmetry for orientation and curvature discrimination, both of which have been proposed as building blocks for global shape representations (see Loffler, 2008, for review), this suggests the emergence of a lower VF advantage for contour shape processing that is absent for its constituent parts.

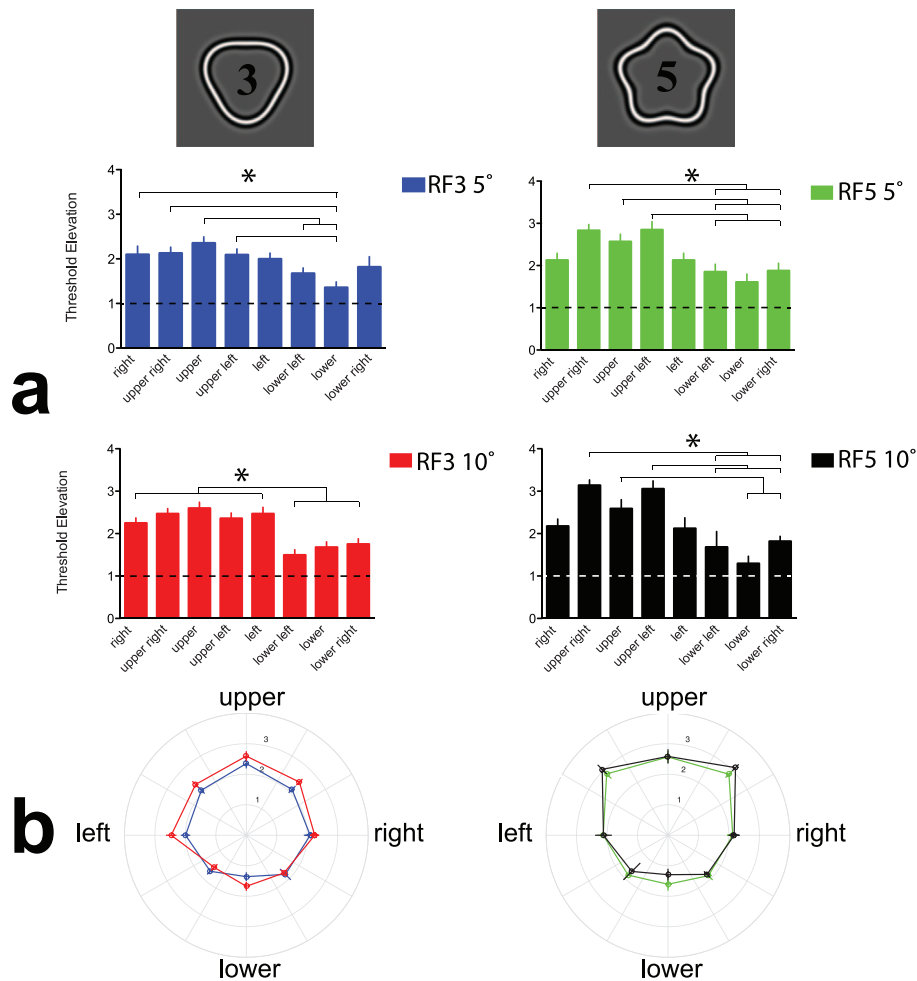


Figure 3. Midlevel task: Shape discrimination at various peripheral locations. Shape discrimination was measured for RF patterns (sinusoidal modulation of the radius of a circular contour given in polar coordinates; see Materials and methods) with frequencies of three and five (see insets) on six observers. Observers had to indicate which of two sequentially presented shapes was noncircular and the minimum amplitude of the RF pattern at which observers performed at 75% correct was used to describe sensitivity. Absolute sensitivity showed a dependence on shape with higher absolute thresholds for an RF3 than RF5, $F(1, 20) = 70.381$; $p < 0.001$. This dependence of discrimination thresholds on RF is in agreement with previous results (Schmidtman et al., 2012). Presenting data as threshold elevations relative to performance for central targets shows a striking similarity for different shapes and eccentricities. Data for the main horizontal, vertical, and diagonal meridians are shown for an RF3 shape at 5° (blue) and 10° (red) as well as for an RF5 shape at 5° (green) and 10° (black) eccentricity in (a) as bar plots and in (b) as polar plots. Differences between individual VF locations that reached statistical significance (Bonferroni post hoc tests) are shown by asterisks.

High-level task: Face discrimination

A hierarchical model of visual processing in the ventral stream assumes that more complex representations are built upon the outputs of comparatively simpler analyzers at low-level locations (Loffler, 2008; Loffler et al., 2003; Schmidtman et al., 2012). Within this framework, face coding would utilize information from units tuned to contour shape, providing, for example, the overall head shape as well as units responding to facial features. As a differential effect of VF location for contour shape processing is evident from Figure 3, this raises the question as to whether a

similar pattern is observed for face discrimination, given its hierarchical higher level of processing compared to shapes. On the other hand, superior performance for face discrimination in the lower VF would not be supported from an evolutionary perspective. Although it is reasonable to argue in favor of an evolutionary drive that results in superior sensitivity to contour shapes in the lower VF (Previc, 1990), such a drive is not obvious for faces.

Face discrimination sensitivity was measured in central vision and at 10° eccentricity in the upper, right, lower, and left peripheral VFs. The stimuli were synthetic faces (Wilson et al., 2002), which isolate the

salient geometrical information (e.g., head shape, hairline, internal feature positions, and shapes) from face photographs. These synthetic faces have been shown to engage the same cortical regions as face photographs and trigger similar activation (Loffler, Yourganov, Wilkinson, & Wilson, 2005). Following initial training with the mean face, observers had to indicate which interval contained the target identity face (nonmean face), which differed from the learned mean face by a variable amount. Sensitivity was defined as the minimum amount of variation required for target faces to be accurately discriminated from the mean face. Discrimination thresholds were also measured for conditions in which the stimuli contained only a subset of the face features: external features (head shape and hairline), internal features (eyes, eyebrows, nose, and mouth), and isolated head shape (i.e., head contour without hairline or any of the internal face features; see insets in Figure 4).

In general, discrimination thresholds were considerably increased for peripheral, relative to central, viewing (Figure 4). For example, peripheral discrimination thresholds for full faces were on average 2.5 times larger than those measured centrally. In addition, threshold elevations depended strongly on VF location, $F(4, 8) = 172.734$; $p < 0.001$, and face features, $F(3, 6) = 46.530$; $p < 0.001$. Threshold elevations for internal features were considerably larger than those for external features. This implies that internal feature discrimination sensitivity is disproportionately reduced in peripheral vision. This is in line with the observation that discrimination of internal face features is dependent upon the resolution of the fine spatial relationships between the component features, and this is reduced peripherally. External features, on the other hand, can be distinguished based on global distortions to the outer face contour.

Importantly, the reduction in sensitivity to face information in peripheral vision was not uniformly distributed. This is evident from the asymmetrical shape of the polar plots in Figure 4b and c. Moreover, there was a highly significant interaction between VF location and face features, $F(12, 24) = 17.659$; $p < 0.001$. Discrimination thresholds for both full faces and internal features were significantly elevated from baseline in the upper, right, and lower VFs ($p < 0.05$, asterisks in Figure 4a). This is not seen for the left VF. Sensitivity to full faces and internal features was greatest in the left VF, relative to all other peripheral VF locations. Although the differences did not reach significance, the data for external features followed the same pattern. In sum, these results indicate that sensitivity to face information in peripheral vision is highest in the left VF.

The pattern of peripheral sensitivity for head shapes was qualitatively different. This is illustrated by the

different shape of the polar plot for head shapes (black contour in Figure 4c). Discrimination thresholds for head shapes were lowest in the lower VF. Data are significantly ($p < 0.05$, asterisks in Figure 4a) elevated from baseline in all peripheral locations except for the lower VF (i.e., sensitivity to head shapes is greatest there). This mirrors the results for shape discrimination (Figure 3). Unlike the set of external face features with a hairline, isolated head shapes bear no obvious resemblance to a face. Accordingly, head shapes may not be treated by the visual system in the same way as full faces. If head shapes fail to engage face-specific mechanisms and were instead processed by more general shape-processing mechanisms, one would expect to see the same pattern of results as for other contour shapes (Figure 3).

Discussion

Performance on visual tasks typically reduces with increasing eccentricity (Strasburger et al., 2011). How this reduction is related to the location of the stimuli within the VF is less clear. Although higher efficiency for visuomotor control, including reaching and grasping, has been shown for the lower VF (Dancerk & Goodale, 2003; Previc, 1990; Rossit et al., 2013), a lower VF advantage has not been found for passive viewing when action was not required (Rossit et al., 2013). Moreover, the lower VF preference seen for visuomotor control is in contrast to behavioral studies, in which performance is typically best along the horizontal (left and right VF; HVA) compared to the vertical meridian with poorest sensitivity in the upper VF (VMA) (Abrams et al., 2012). This leaves open the question as to what the enhanced reaching and grasping performance relies upon and why a lower VF advantage may not manifest for visual perception tasks. The aim of this study was to address these issues by systematically investigating visual sensitivity for stimuli of increasing complexity at various locations and eccentricities within the peripheral VF.

Our data show differing profiles of peripheral VF sensitivities for different stimuli. Orientation and curvature discrimination show isotropic behavior with similar sensitivities along the vertical and horizontal meridians. Closed contour shapes, on the other hand, show a lower VF preference with higher sensitivity along all tested locations in the lower VF. Finally, faces are best discriminated when they are presented in the left VF. The dependence of the peripheral sensitivity profile on the stimulus has not been reported previously. Most earlier studies have focused on a specific task and stimulus. Our systematic investigation shows

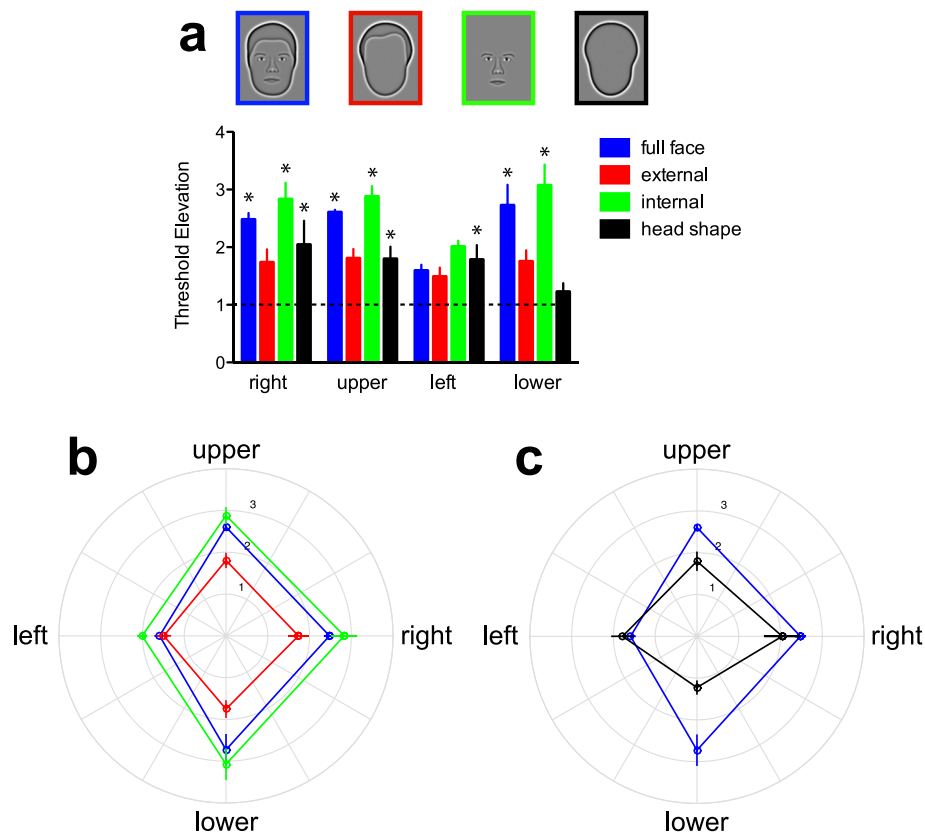


Figure 4. High-level task: Face discrimination at various peripheral locations. Various aspects of face discrimination sensitivity were measured in five VF locations (central, upper, right, lower, and left) for four types of face features (full faces, external features, internal features, and head shapes; see insets). Three observers had to indicate which of two sequentially presented faces was the target face that deviated from a learned mean face (reference) by a variable amount (see Materials and methods). Face sensitivity was defined as the minimum variation between reference and target required for reliable discrimination. (a) Data are presented as threshold elevations, relative to baseline (central viewing). Data are averaged across four face identities, presented randomly in an interleaved design. Threshold elevations depended strongly on both VF location and face features. For full faces and internal features, discrimination thresholds were significantly elevated from baseline (central viewing) in the upper, right, and lower VF (post hoc comparisons with Bonferroni correction; $p < 0.05$, asterisks). Peripheral threshold elevations were considerably lower in the left VF. The same pattern of results was evident for external features although the differences did not reach significance. A different pattern is seen for head shapes: threshold elevations were significant in the upper, right, and left VF ($p < 0.05$). Peripheral head shape discrimination sensitivity was highest in the lower visual field. (b, c) The data presented as polar plots. (b) Sensitivity for full faces (blue), external features (red), and internal features (green) is highest in the left VF (i.e., closest to origin). (c) A different pattern of peripheral sensitivity for head shapes is evident in the deviation of the shape of the associated profile (black line) from that for the full face (blue, replotted from [b]). Sensitivity for head shapes is maximal in the lower VF in agreement with the data for single RF shapes (Figure 3).

that, for the same observers and under comparable experimental conditions, the patterns of performance across the VF differs for different stimuli. Furthermore, the general advantage for the lower VF for shape discrimination is at odds with both the VMA and HVA. HVA would predict that performance along the horizontal meridian is superior to other iso-eccentric visual field locations (HVA) (Abrams et al., 2012). VMA would predict better performance in the lower compared to upper VF, but this should be restricted to the vertical axis (Abrams et al., 2012). We see best performance in the lower VF—inconsistent with

HVA—extending up to at least $\pm 45^\circ$ from the vertical, which is inconsistent with VMA.

The lower VF preference may be independent of the precise shape. The same VF advantage is seen for two different simple shapes (RF3 and RF5). As faces show a different pattern of results with highest sensitivity in the left VF, this offered the opportunity to use head shapes (removing all other face features) to investigate if the lower VF advantage might be a feature of shapes in general or if it is limited to simple, perhaps symmetrical, shapes, such as triangles or pentagons. If lower VF advantage were a general feature for shapes,

a higher sensitivity in the lower VF should be recovered when removing the internal features from the faces. As this turned out to be the case, it provides evidence in support of the hypothesis that the pattern of higher sensitivity in the lower VF may be a feature of shapes in general. This is further corroborated by the fact that symmetry is not a requirement. First, a lower VF advantage is obtained in the absence of bilateral symmetry. Although the simple RF shapes contain symmetry (three symmetry axes for an RF3 and five for an RF5), given that they were presented with random phases (orientations), the shapes would typically not be bilaterally symmetric. Second, head shapes that lack symmetry altogether give the same pattern of results. The head outlines were composed of the combination of seven RF patterns with different frequencies, amplitudes, and phases and lacked symmetry. Hence, symmetry, bilateral or otherwise, can be ruled out as a critical factor for the lower VF advantage in peripheral shape discrimination. Together, the results are consistent with a pattern of peripheral sensitivity that is seen for a wide range of shapes. It remains for future studies to investigate what shape aspects might limit the observed greater sensitivity in the lower VF observed here.

Following the proposed hierarchical processing of visual information in the ventral stream, the present study quantified performance for stimuli of increasing complexity to determine how sensitivity depends on VF location. This allows differentiation between two hypotheses. First, assuming a strictly feed-forward hierarchical model of visual processing, any anisotropy would carry forward into the next stage, i.e., any pattern of VF specialization (e.g., superior performance for the horizontal meridian) at a specific cortical level would also be expected for processing at subsequent, higher levels. Hence, if VF asymmetries existed for low-level stimuli, such as contour orientation, a strictly feed-forward hierarchical model would predict that these asymmetries would also be evident for more complex stimuli, such as extended shapes and objects. Alternatively, VF specialization may be task-specific, and, for example, a lower VF advantage may be present only for those tasks that serve specific visually guided actions, such as visual perception of contour shape to facilitate fine motor control for, e.g., grasping.

We find a significant VF asymmetry with a lower VF advantage for midlevel shape discrimination that is absent for putative lower-level (orientation and curvature discrimination) as well as higher-level tasks (face discrimination). These results are inconsistent with a narrow interpretation of a feed-forward model of visual processing. Current models of object recognition (Cadiou et al., 2007; Riesenhuber & Poggio, 2000; Serre, Oliva, & Poggio, 2007; Van Essen et al., 1992) assume that the neuronal encoding of shapes and

objects is achieved by a modular architecture along the ventral pathway (Goodale & Milner, 1992; Ungerleider & Mishkin, 1982), a hypothesis based on the increasing receptive field sizes, increasing invariance to position and scale, and increasing stimulus complexity for which neurons along this pathway show selectivity (Logothetis et al., 1995; Tanaka & Kobatake, 1994).

Following anatomical and physiological evidence in support of the existence and importance of feedback and/or lateral connections (Lamme & Roelfsema, 2000; Lamme, Supèr, & Spekreijse, 1998), it is generally acknowledged that a strictly feed-forward structure is likely too simplistic to account for the complexity of visual processing. Although it remains to be seen what the precise functional role of feedback is and how this impacts on the design of models, it is evident that our data will provide a challenge for future models. A successful model would have to explain why low-level features, such as orientation and curvature, exhibit an isotropic behavior whereas simple (RF contours) as well as complex (head outlines) shapes show lower VF preference that, in turn, is not evident for face stimuli. In the absence of a current model that predicts our results, our data provide a critical test for any model that spans various processing stages along the ventral pathway.

Our data are inconsistent with a strictly feed-forward model of visual processing under the assumption that high-level processes (e.g., as assessed by face discrimination) receive inputs from midlevel (e.g., shape) computation. One might, however, question whether face discrimination is representative of higher-level processing more generally. A substantial body of evidence suggests that faces may constitute a special class of visual objects processed at a high-level of the ventral stream (see McKone & Robbins, 2011, for a review). This leaves the possibility, then, that, for other higher-level tasks that might be processed in a fundamentally different way from faces, the pattern of peripheral VF sensitivity may be more similar to that seen for closed shapes. The finding of different VF biases for shape and face discrimination may therefore not unequivocally challenge models based on hierarchical processing stages. It remains for future studies to investigate whether the pattern of peripheral sensitivity is dependent on a particular high-level task, for example, discrimination between body parts (hands or feet), animals, or artifacts. These could potentially add further insight into hierarchical versus task-specific strategies of visual processing and inform detailed models of the ventral stream.

The emergence of a lower VF advantage for shape discrimination is likely caused by processing in the extrastriate cortex. Anatomically, cone and ganglion cell density at the retina are highest along the horizontal meridian and higher in the upper retina

(lower VF) compared to the lower retina (upper VF) (Curcio & Allen, 1990; Perry, Oehler, & Cowey, 1984). These anatomical asymmetries have been linked to better performance along the horizontal compared to vertical meridian (HVA) and the perceptual asymmetry along the vertical axis (VMA) (Abrams et al., 2012). Physiological correlates for the VMA have been reported in the early stages of cortical processing. Studies employing fMRI (Liu et al., 2006) and MEG (Portin et al., 1999) studies have reported higher activation to stimulation in the lower compared to upper part of the vertical meridian in V1/V2.

Neither of these observations, however, would predict a specialized lower VF superiority that is unique to shape discrimination. Evidence from behavioral (Loffler, 2008; Loffler et al., 2003; Schmidtman et al., 2012; Wilkinson et al., 1998), neurophysiological (Gallant et al., 1996; Hegdé & Van Essen, 2007; Pasupathy & Connor, 2002; Yau et al., 2009), and imaging (Dumoulin & Hess, 2007; Wilkinson et al., 2000) studies converge in favor of an extrastriate locus, possibly V4 or the lateral occipital complex, specialized for shape processing (Loffler, 2008). Given the lower VF advantage for shapes and the absence of a VF asymmetry for curvature and orientation discrimination, this suggests that the asymmetries have their origin in these extrastriate areas. Our results make interesting and testable predictions for future studies investigating neuronal sensitivity to different VF locations within these extrastriate regions. Future studies are required to determine if the observed lower VF advantage for shapes may be due to anatomical or physiological differences in, e.g., V4 for different VF locations.

Face discrimination shows a different pattern. Rather than a lower VF advantage, a significant left VF bias was found. This is consistent with the established left-over-right VF advantage for face processing (Leehey et al., 1978; Young et al., 1985). The left-over-right effect has been linked to the right hemifield lateralization of the highly face-sensitive fusiform face area (FFA; Kanwisher & Yovel, 2006). Our results extend this to include the vertical meridian: Face discrimination sensitivity is greatest in the left compared to all other meridians, including the upper, right, and lower VF. A comparable left VF advantage was also found when observers were presented with isolated internal (eyes, brows, mouth, and nose) or external (head shape and hairline) face features. These results indicate that sensitivity to face information is greatest in the left VF, which is in line with Yovel, Tambini, and Brandman (2008), who reported that the magnitude of the left VF advantage for face discrimination is strongly correlated with the enhanced size of the right, relative to left FFA. A different topography of peripheral sensitivity was identified for head shapes by

further removing the hairline from the external face features. In contrast to the left VF advantage, head shape sensitivity was greatest in the lower VF. This lower VF advantage for head shape mirrors that for simple shapes (Figure 3). The dramatic effect of the hairline in modulating the pattern of VF sensitivity is striking. The lower and left VF advantage for head shapes and faces, respectively, is suggestive of a qualitative distinction between the processing of faces and shapes, including head outlines.

Our results provide a novel link between enhanced visually guided movement in the lower VF and visual perception. The topography of peripheral VF sensitivity for contour shapes is not the result of a lower level effect nor does it appear to cause an effect at higher levels. A different pattern of VF sensitivity is seen for constituent shape parts, as measured by orientation and curvature discrimination, as well as for complex objects that contain contour shape. A lower VF advantage that is specific to shape processing argues in favor of a task-specific effect, which may have evolved to serve visually guided manipulation of natural shapes in peri-personal space (Danckert & Goodale, 2003; Previc, 1990; Rossit et al., 2013). This is pragmatic from an evolutionary point of view: Humans most frequently manipulate objects that appear first in their lower VF and, therefore, benefit from higher sensitivity to the overall shape of these objects in order to reach and grasp for them (Previc, 1990). That these hemifield asymmetries do not appear to transfer to more complex, higher-level tasks, such as face discrimination, is consistent with a task-specific hypothesis. A lower VF advantage is of benefit for the manipulation of objects, which may heavily rely on the visual processing of general contour information but not for more complex tasks, such as face recognition.

Keywords: orientation discrimination, curvature discrimination, peripheral vision, spatial vision, shape perception, face perception, vertical meridian asymmetry, horizontal vertical anisotropy

Acknowledgments

Commercial relationships: none.

Corresponding authors: Gunnar Schmidtman, Andrew J. Logan, Gunter Loffler.

Email: Gunnar.schmidtman@mcgill.ca;

A.Logan@bradford.ac.uk; g.loffler@gcu.ac.uk.

Address: McGill Vision Research, Department of Ophthalmology, McGill University, Montreal, QC, Canada (GS); Department of Life Sciences, Glasgow Caledonian University, Glasgow, UK (AJL and GL).

Footnote

¹ We will use the term “contour parts” to refer to local information about an object’s contour outline, i.e., its orientation or curvature at a specific point. “Object shape” will be used to describe the overall shape given by the outline of an object. An “object” (or “complex object”) is a stimulus that contains information about shape but also about, e.g., texture, shading, depth, color, position of features, etc. For example, a face is considered an “object” that has a certain “shape” (e.g., elliptical) and features (e.g., eyes). “Contour parts” refers to different positions on the “shape” with, e.g., points of high curvature around the chin line.

References

- Abrams, J., Nizam, A., & Carrasco, M. (2012). Isoeccentric locations are not equivalent: The extent of the vertical meridian asymmetry. *Vision Research*, 52(1), 70–78.
- Adams, D. L., & Horton, J. (2003). A precise retinotopic map of primate striate cortex generated from the representation of angioscotomas. *The Journal of Neuroscience*, 23(9), 3771–3789.
- Cadiou, C., Kouh, M., Pasupathy, A., Connor, C. E., Riesenhuber, M., Poggio, T., & Pasupathy, A. (2007). A model of V4 shape selectivity and invariance. *Journal of Neurophysiology*, 98(3), 1733–1750.
- Carandini, M., & Heeger, D. J. (2011). Normalization as a canonical neural computation. *Nature Reviews Neuroscience*, 13, 51–62.
- Connolly, M., & Van Essen, D. (1984). The representation of the visual field in parvicellular and magnocellular layers of the lateral geniculate nucleus in the macaque monkey. *Journal of Comparative Neurology*, 226(4), 544–564.
- Curcio, C. A., & Allen, K. A. (1990). Topography of ganglion cells in human retina. *Journal of Comparative Neurology*, 300(1), 5–25.
- Curcio, C. A., Sloan, K. R., Packer, O., Hendrickson, A. E., & Kalina, R. E. (1987). Distribution of cones in human and monkey retina: Individual variability and radial asymmetry. *Science*, 236(4801), 579–582.
- Danckert, J., & Goodale, M. A. (2003). Ups and downs in the visual control of action. In S. H. Johnson-Frey, (Ed.), *Cognitive neuroscience perspectives on intentional acts* (pp. 29–64). MIT Press: Cambridge, MA.
- Davey, M. P., & Zanker, J. M. (1998). Detecting the orientation of short lines in the periphery. *Australian and New Zealand Journal of Ophthalmology*, 26(Suppl.), 104–107.
- De Valois, R. L., Yund, E. W., & Hepler, N. (1982). The orientation and direction selectivity of cells in macaque visual cortex. *Vision Research*, 22(5), 531–544.
- Dumoulin, S., & Hess, R. F. (2007). Cortical specialization for concentric shape processing. *Vision Research*, 47(12), 1608–1613.
- Gallant, J., Braun, J., & Van Essen, D. C. (1993). Selectivity for polar, hyperbolic, and Cartesian gratings in macaque visual cortex. *Science*, 259(5091), 100–103.
- Gallant, J. L., Connor, C. E., Rakshit, S., Lewis, J. W., & Van Essen, D. C. (1996). Neural responses to polar, hyperbolic, and Cartesian gratings in area V4 of the macaque monkey. *Journal of Neurophysiology*, 76(4), 2718–2739.
- Goodale, M., & Milner, A. (1992). Separate visual pathways for perception and action. *Trends Neurosci*, 15(1), 20–25.
- Hay, D. C. (1981). Asymmetries in face processing: Evidence for a right hemisphere perceptual advantage. *The Quarterly Journal of Experimental Psychology. A, Human Experimental Psychology*, 33, 267–274.
- Hegd , J., & Van Essen, D. C. (2000). Selectivity for complex shapes in primate visual area V2. *Journal of Neuroscience*, 20(5), RC61.
- Hegd , J., & Van Essen, D. C. (2007). A comparative study of shape representation in macaque visual areas V2 and V4. *Cerebral Cortex*, 17(5), 1100–1116.
- Hubel, D. H., & Wiesel, T. N. (1962). Receptive fields, binocular interaction and functional architecture in the cat’s visual cortex. *Journal of Physiology*, 160, 106–154.
- Hubel, D. H., & Wiesel, T. N. (1968). Receptive fields and functional architecture of monkey striate cortex. *Journal of Physiology*, 195(1), 215–243.
- Ito, M., & Komatsu, H. (2004). Representation of angles embedded within contour stimuli in area V2 of macaque monkeys. *Journal of Neuroscience*, 24(13), 3313–3324.
- Kanwisher, N., & Yovel, G. (2006). The fusiform face area: A cortical region specialized for the perception of faces. *Philosophical Transactions of the Royal Society of London. Series B, Biological Sciences*, 361(1476), 2109–2128.
- Lamme, V. A., & Roelfsema, P. R. (2000). The distinct

- modes of vision offered by feedforward and recurrent processing. *Trends in Neuroscience*, 23(11), 571–579.
- Lamme, V. A., Supèr, H., & Spekreijse, H. (1998). Feedforward, horizontal, and feedback processing in the visual cortex. *Current Opinion in Neurobiology*, 8(4), 529–535.
- Leehey, S., Carey, S., Diamond, R., & Cahn, A. (1978). Upright and inverted faces: The right hemisphere knows the difference. *Cortex*, 14(3), 411–419.
- Levi, D. M., Klein, S. A., & Aitsebaomo, P. (1985). Vernier acuity, crowding and cortical magnification. *Vision Research*, 25(7), 963–977.
- Liu, T., Heeger, D. J., & Carrasco, M. (2006). Neural correlates of the visual vertical meridian asymmetry. *Journal of Vision*, 6(11):12, 1294–1306, <http://www.journalofvision.org/content/6/11/12>, doi:10.1167/6.11.12. [PubMed] [Article]
- Loffler, G. (2008). Perception of contours and shapes: Low and intermediate stage mechanisms. *Vision Research*, 48(20), 2106–2127.
- Loffler, G. (2015). Probing intermediate stages of shape processing. *Journal of Vision*, in press.
- Loffler, G., Wilson, H. R., & Wilkinson, F. (2003). Local and global contributions to shape discrimination. *Vision Research*, 43(5), 519–530.
- Loffler, G., Yourganov, G., Wilkinson, F., & Wilson, H. R. (2005). fMRI evidence for the neural representation of faces. *Nature Neuroscience*, 8(10), 1386–1390.
- Logothetis, N. K., Pauls, J., & Poggio, T. (1995). Shape representation in the inferior temporal cortex of monkeys. *Current Biology*, 5(5), 552–563.
- Maunsell, J., & Newsome, W. T. (1987). Visual processing in monkey extrastriate cortex. *Annual Review of Neuroscience*, 10, 363–401.
- McKone, E., & Robbins, R. (2011). Are faces special? In A. Calder, G. Rhodes, M. Johnson, & J. Haxby (Eds.), *Oxford handbook of face perception* (pp. 149–176). Oxford, UK: Oxford University Press.
- Näsänen, R. (1999). Spatial frequency bandwidth used in the recognition of facial images. *Vision Research*, 39(23), 3824–3833.
- Pasupathy, A., & Connor, C. E. (2002). Population coding of shape in area V4. *Nature Neuroscience*, 5(12), 1332–1338.
- Pelli, D. G. (1997). The VideoToolbox software for visual psychophysics: Transforming numbers into movies. *Spatial Vision*, 10(4), 437–442.
- Perry, V. H., Oehler, R., & Cowey, A. (1984). Retinal ganglion cells that project to the dorsal lateral geniculate nucleus in the macaque monkey. *Neuroscience*, 12(4), 1101–1123.
- Phillips, G. C., & Wilson, H. R. (1984). Orientation bandwidths of spatial mechanisms measured by masking. *Journal of the Optical Society of America*, 1(2), 226–232.
- Portin, K., Vanni, S., & Virsu, V. (1999). Stronger occipital cortical activation to lower than upper visual field stimuli neuromagnetic recordings. *Experimental Brain Research*, 124, 287–294.
- Previc, F. H. (1990). Functional specialization in the lower and upper visual fields in humans: Its ecological origins and neurophysiological implications. *Behavioural Brain Research*, 13, 519–541.
- Riesenhuber, M., & Poggio, T. (2000). Models of object recognition. *Nature Neuroscience*, 3, 1199–2000.
- Rossit, S., McAdam, T., Mclean, D. A., Goodale, M. A., & Culham, J. C. (2013). fMRI reveals a lower visual field preference for hand actions in human superior-parietal occipital cortex (SPOC) and precuneus. *Cortex*, 49(9), 2525–2541.
- Rubin, N., Nakayama, K., & Shapley, R. (1996). Enhanced perception of illusory contours in the lower versus upper visual hemifields. *Science*, 271(5249), 651–653.
- Schmidtman, G., Kennedy, G. J., Orbach, H. S., & Loffler, G. (2012). Non-linear global pooling in the discrimination of circular and non-circular shapes. *Vision Research*, 62, 44–56.
- Serre, T., Oliva, A., & Poggio, T. (2007). A feedforward architecture accounts for rapid categorization. *Proceedings of the National Academy of Sciences, USA*, 104(15), 6424–6429.
- Skrandies, W. (1985). Human contrast sensitivity: Regional retinal differences. *Human Neurobiology*, 4(2), 97–99.
- Strasburger, H., Rentschler, I., & Jüttner, M. (2011). Peripheral vision and pattern recognition: A review. *Journal of Vision*, 11(5):13, 1–82, <http://www.journalofvision.org/content/11/5/13>, doi:10.1167/11.5.13. [PubMed] [Article]
- Tanaka, K., & Kobatake, E. (1994). Neuronal selectivities to complex object features in the ventral visual pathway of the macaque cerebral cortex. *Journal of Neurophysiology*, 71(3), 856–867.
- Tootell, R. B. H., Hadjikhani, N. K., Vanduffel, W., Liu, A. K., Mendola, J. D., Sereno, M. I., & Dale, A. M. (1998). Functional analysis of primary visual cortex (V1) in humans. *Proceedings of the National Academy of Sciences, USA*, 95, 811–817.
- Tsao, D. Y., & Livingstone, M. S. (2008). Mechanisms

- of face perception. *Annual Review of Neuroscience*, 31, 411–437.
- Ungerleider, L. G., & Mishkin, M. (1982). Two cortical visual systems. In D. J. Ingle, M. A. Goodale, & R. J. W. Mansfield, (Eds.), *Analysis of visual behavior* (pp. 549–586). Cambridge, MA: MIT Press.
- Van Essen, D. C., Anderson, C., & Felleman, D. (1992). Information processing in the primate visual system: An integrated systems perspective. *Science*, 255(5043), 419–423.
- Van Essen, D. C., Newsome, W. T., & Maunsell, J. H. R. (1984). The visual field representation in striate cortex of the macaque monkey: Asymmetries, anisotropies, and individual variability. *Vision Research*, 24(5), 429–448.
- Wilkinson, F., James, T. W., Wilson, H. R., Gati, J. S., Menon, R. S., & Goodale, M. A. (2000). An fMRI study of the selective activation of human extrastriate form vision areas by radial and concentric gratings. *Current Biology: CB*, 10(22), 1455–1458.
- Wilkinson, F., Wilson, H. R., & Habak, C. (1998). Detection and recognition of radial frequency patterns. *Vision Research*, 38(22), 3555–3568.
- Wilson, H. R., Loffler, G., & Wilkinson, F. (2002). Synthetic faces, face cubes, and the geometry of face space. *Vision Research*, 42, 2909–2923.
- Yau, J. M., Pasupathy, A., Fitzgerald, P. J., Hsiao, S. S., & Connor, C. E. (2009). Analogous intermediate shape coding in vision and touch. *Proceedings of the National Academy of Sciences, USA*, 106(38), 16457–16462.
- Young, A. W., Hay, D. C., McWeeny, K. H., Ellis, A. W., & Barry, C. (1985). Familiarity decisions for faces presented to the left and right cerebral hemispheres. *Brain and Cognition*, 4(4), 439–450.
- Yovel, G., Tambini, A., & Brandman, T. (2008). The asymmetry of the fusiform face area is a stable individual characteristic that underlies the left-visual-field superiority for faces. *Neuropsychologia*, 46(13), 3061–3068.